Broadband dielectric spectroscopy of a nematic liquid crystal in benzene

Shyamal Kumar Kundu,[a] Shun Okudaira, Masanori Kosuge, Naoki Shinyashiki, and Shin Yagihara[b]
Department of Physics, School of Science, Tokai University, 1117, Kitakaname, Hiratsuka, Kanagawa 259-1292, Japan

(Received 23 July 2008; accepted 10 September 2008; published online 27 October 2008)

Broadband dielectric spectroscopy has been used to analyze the temperature, frequency, and concentration dependences of the molecular dynamics of a nematic liquid crystal (5CB) mixed with the nonpolar solvent benzene. Differential scanning calorimetry measurement has been also performed to confirm the phase transitions of 5CB/benzene mixtures. The phase transition temperatures (crystalline to isotropic phases) thus obtained have been described very accurately from the temperature-dependent relaxation strength, the relaxation time, and the symmetric shape parameter of the relaxation function obtained from the fitting procedure. Two relaxation processes reflecting overall rotations around the short and long molecular axes are observed in both the nematic and isotropic phases. In the crystalline phase, the former process with the longer relaxation time disappeared, and latter process with shorter relaxation time shows a discontinuity at the freezing temperature. The relaxation process with shorter relaxation time obtained in the crystalline phase is larger than that obtained in the nematic phase because of the large restrictions in the crystalline phase. For the first time, we have precisely explained the molecular mechanism and structure of liquid crystalline materials as a function of concentration, temperature, and frequency. © *2008 American Institute of Physics*. [DOI: 10.1063/1.2993255]

INTRODUCTION

Confined and dispersed soft condensed matter has been a field of active research for more than a decade, which has attracted the attention of scientists either looking for fundamental changes in the physical properties of materials or searching for new applications.[1–6] The behavior of a bulk nematic liquid crystal (NLC) in the presence of an external field is of importance for many technical applications as well as basic physical research.[7–9] A study of the dynamic microstructure of liquid crystals (LCs) is very essential to solve recent problems about properties of matter of the liquid crystals. This is because the properties of matter of liquid crystals reflect not only chemical structure of one molecule but also various molecular arrangements and structure of a domain. The dielectric anisotropy of NLCs plays an important role in the applications of the electrical effect to display devices and spatial modulators.[10] The most fundamental problems of predicting physical properties of liquid crystalline compounds are based upon information on molecular shape and intermolecular interactions. A small change in molecular structure can result in a dramatic change in the corresponding liquid crystal properties.

Jadzyn *et al.*[11] showed a pretransitional critical-like behavior of dielectric permittivity in the mixtures of mesomorphic and nonmesomorphic compounds. Usol'tseva *et al.*[12] showed that dissolving a thermotropic liquid crystal compound into nonpolar organic solvent could produce ferroelectric LCs with remarkable properties. The electrooptic switching properties of the solutions are, to some extent, better than those of the pure LCs.[13] Cinacchi[14] studied a molecular dynamics simulation on the liquid-crystalline binary mixture formed by discogen hexakis-pentyloxytriphenylene (solvent), and benzene (solute), and they observed that the confinement in a columnar discotic liquid-crystalline matrix largely affected the translational and rotational dynamics of benzene. However, the fundamental properties and the dynamics structure of LCs at a molecular level have not been clarified yet because of the lack of analysis of the experimental data and understanding of the connection between microscopic molecular dynamics and those of collective dynamics.

The motivation of this work is to study the molecular dynamics of a NLC in nonpolar solvent, benzene. We used broadband dielectric spectroscopy (BDS) and differential scanning calorimetry (DSC) techniques to investigate the phase transitions, relaxation mechanism and intermolecular interactions of a NLC mixed with benzene. Dielectric spectroscopic techniques including especially high frequency up to 30 GHz are effective to examine fast dynamics such as local motions of polymers and liquid crystals. We will show that phase transition temperatures are described very accurately from the temperature-dependent relaxation parameters (e.g., dielectric strength, relaxation frequency, and shape parameter) obtained from the fitting procedure of Eq. (1).

[a]Present address: Institute for Solid State Physics, The University of Tokyo, 5-1-5 Kashiwanoha, Kashiwa, Chiba, Japan. Electronic mail: kundu05@gmail.com.
[b]Author to whom correspondence should be addressed. Electronic mail: yagihara@keyaki.cc.u-tokai.ac.jp.

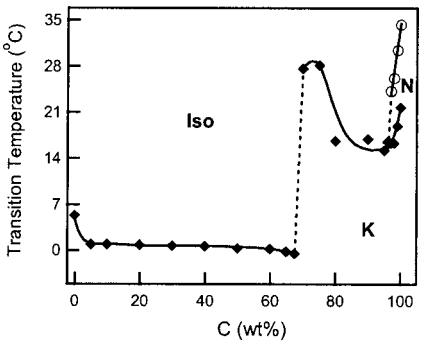

FIG. 1. (a) Transition temperature-concentration phase diagram of 5CB/benzene mixture obtained from DSC. K, N, and Iso correspond to the crystallization, nematic, and isotropic phases, respectively. The lines are drawn as a guide for the eye.

EXPERIMENTAL

Although, the dielectric properties of the bulk alkylcyanobiphenyls have been studied extensively,[15–21] we will use a NLC as 4′pentyl-4-biphenylcarbonitrile(5CB) for the simple structure and for simplicity of the present discussion. The LC material, 5CB, was purchased from Sigma-Aldrich, Japan. Benzene with pure grade was purchased from Wako Pure Chemical Industries, Japan. These were used without further purification. 5CB/benzene mixtures with different concentrations of 5CB (e.g., $10,20,\ldots,100$ wt. %) were used for DSC and BDS measurements. The BDS measurements were carried out by two subsystems: time domain reflectometer (TDR) (Hewlett Packard 54210B), having a frequency range of 100 MHz–30 GHz and impedance analyzer (Agilent Technology HP4294A) having a frequency range of 40 Hz–110 MHz. During the dielectric measurements, the sample temperature was varied between −10 and 40 °C. A coaxial-cylindrical cell with the inner conductor diameter (made by platinum) of 2 mm and the outer conductor (gold plated stainless still) inner diameter of 3.5 mm was used for both TDR and impedance analyzer systems of dielectric measurements. The lengths of the inner and outer conductor were 5 and 23.7 mm, respectively, and the electric cell length was approximately 6.65 mm.

The DSC measurements were made with differential scanning calorimeter (Seiko SSC/5200H DSC-120). The DSC measurements were performed by heating process from −20 to 70 °C at a scanning rate of 1 °C/min. The sample was kept at −20 °C for about 2 h to ensure the equilibrium before starting data acquisition.

RESULTS AND DISCUSSION

The concentration-temperature (C-T) phase diagram obtained from DSC measurement is shown in Fig. 1. Pure 5CB takes a nematic liquid crystalline phase at room temperature because of the anisotropic shape of the rigid molecule. It is seen from Fig. 1 that the crystalline (K)-isotropic (Iso) phase transition temperatures are slightly decreased with increasing concentration of 5CB up to 69 wt %, but at 70 wt % of 5CB, the phase transition temperature abruptly increases to about 27 °C and then decreases of about 15 °C and again increases from 96 to 100 wt % of 5CB. It is clear from Fig. 1 that 70 wt % of 5CB is the critical concentration, where phase behavior is strongly correlated with the composition of LC and benzene molecules, thus the molecules have strong tendency to form antiparallel correlated pairs. Therefore, in the range of 70–96 wt % of 5CB, the LC molecules dynamically form antiparallel correlated pairs, hence the antiparallel dimers of the LC molecules are builtup.[22–27] Such dimers are viewed as being formed by the bonding of two "monomers," each monomer consisting of a mesogenic core and an end chain of half the spacer length. These pairs are formed more easily in the nematic phase. So the molecular alignments are easily produced above 96 wt % of 5CB to form a NLC phase.

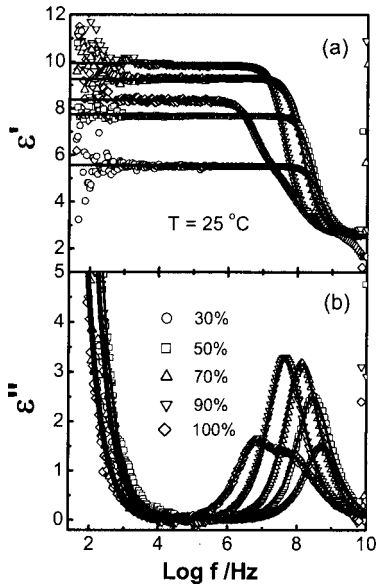

FIG. 2. Variation of the real and imaginary parts of the complex dielectric permittivity with frequency for different concentrations of 5CB/benzene mixture at 25 °C. 30% to 100% corresponds to the concentration of 5CB. Solid curves represent the fitting curves using Eq. (1).

The concentration dependences of the real and imaginary parts of the complex dielectric permittivity ($\varepsilon^*=\varepsilon'-i\varepsilon''$, where ε' and ε'' are, respectively, the real and imaginary parts of the complex dielectric permittivity) measured at a fixed temperature of 25 °C for 5CB/benzene mixture are shown in Fig. 2. To characterize the dielectric relaxation spectrum, curve fitting procedures were carried out. The dielectric constant and loss for the liquid crystalline materials were described from the fitting of the complex dielectric permittivity using[33,34]

$$\varepsilon^*(\omega)-\varepsilon_\infty=\sum_{k=1}^{2}\frac{\Delta\varepsilon_k}{1+(i\omega\tau_k)^{\beta_k}}+\frac{\sigma_{\mathrm{DC}}}{i\omega\varepsilon_0} \tag{1}$$

where $\Delta\varepsilon_k$ is the dielectric relaxation strength, σ_{DC} is the DC conductivity, ε_0 is the dielectric constant in vacuum and ε_∞ is the high-frequency permittivity, $\tau_k(=1/2\pi\nu_k)$ is the relaxation time, ν_k is the characteristic frequency, and β_k is the symmetric shape parameter. $\beta=1$ gives the Debye function and $0<\beta<1$ gives the Cole–Cole function.[35] All the complex dielectric permittivity obtained from the 5CB/benzene mixtures are analyzed well by considering two relaxation processes and DC conductivity. Solid curves, which have

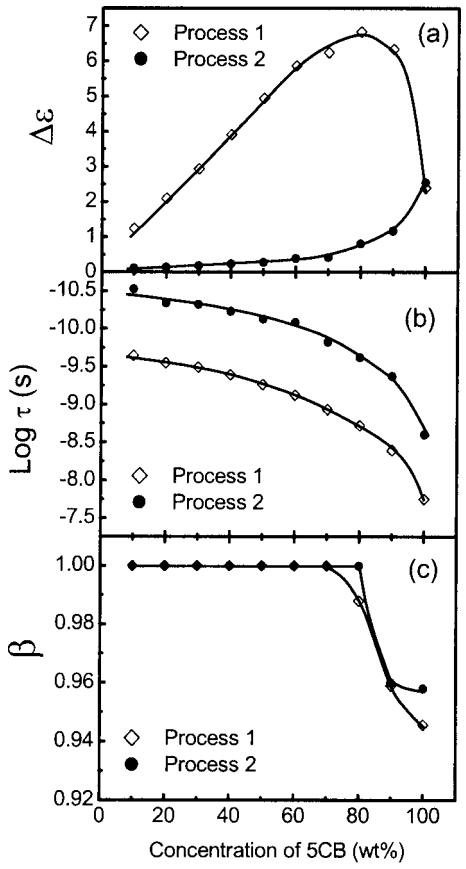

FIG. 3. Concentration dependence of (a) relaxation strength, (b) relaxation time, and (c) distribution parameter for 5CB/benzene mixture at 25 °C. The lines are drawn as a guide for the eye.

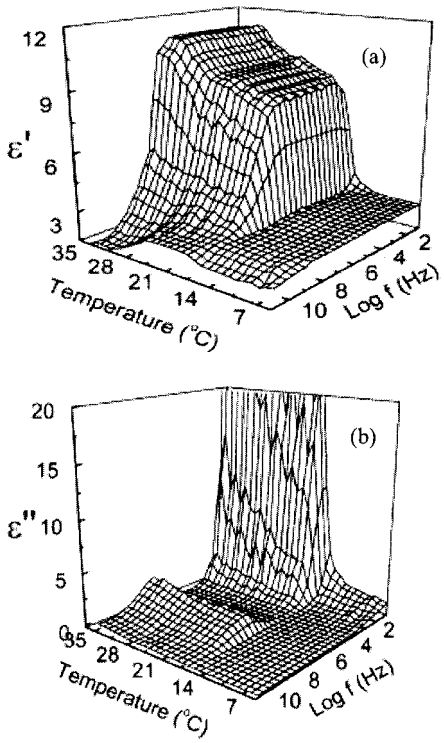

FIG. 4. 3D temperature-frequency plot of the real and imaginary parts of the complex dielectric permittivity for 98 wt % 5CB/benzene mixture.

been shown in Fig. 2, represent the fitting curves using Eq. (1). We have observed two processes, one with a longer relaxation time due to the molecular rotation around the short (l) axis (process 1) and one with a short relaxation time due to the molecular rotation around the long (l) axis (process 2).[28–32] Such molecular rotations have been shown schematically in Fig. 6. Figure 2 also shows the contribution from the DC conductivity which is generally observed in the low-frequency side of the dielectric spectrum for the liquid crystalline materials. It is well known that liquid crystals are not absolutely free from impurities.

Variations of the relaxation parameters obtained from process 1 ($\Delta\varepsilon_1$, τ_1, and β_1) and from process 2 ($\Delta\varepsilon_2$, τ_2, and β_2) with concentration of 5CB/benzene mixture at 25 °C are shown in Fig. 3. Figure 3(a) shows that $\Delta\varepsilon_1$ increases with increasing concentration of 5CB, because the number density of dipoles increases by increasing concentration. But at very high concentration, $\Delta\varepsilon_1$ decreases because the molecules are more ordered and restricted than lower concentrated region and the effective moment decreases. For process 2, $\Delta\varepsilon_2$ increases very slowly below 70 wt % of 5CB and then change of $\Delta\varepsilon_2$ is noticeable. Because, even higher concentrations, the dynamics is not restricted by the small excluded volume effect which is much more effective for the process 1. Figure 3(b) shows that both τ_1 and τ_2 increases with increasing concentration of 5CB. This is because, when the concentration is low, the dipoles are freely rotating around their own axis. By increasing concentration, the interactions between the dipoles increase and the viscosity of the solutions increases which reduces the rate of the rotation of dipoles around their own axis. It should be noted that, if we consider a single 5CB molecule (see the inset of Fig. 6), the ratio along the long and short axes of the 5CB molecule is almost $2\frac{1}{2}$, so that, the difference of τ_1 and τ_2 is appeared to be above 1 decade.[36] Figure 3(c) shows that, in the low concentration region, the dielectric permittivity is explained by Debye function (β=0) but at very high concentration regions ($\geqslant$70 wt % of 5CB), the dielectric permittivity is explained by Cole–Cole function ($0<\beta<1$). At the very high concentration region, the antiparallel dimers of the LC molecules are formed.[22–27] and slow dynamics generally accompany broaden relaxation time.[37]

We have made the dielectric measurements to examine the temperature dependent LC phase transitions at different concentrations and observed the similar nature of the phase transitions obtained from DSC study (Fig. 1). For example, for 98 wt % 5CB/benzene mixture, we have measured the temperature dependence of the complex dielectric permittivity using BDS. Figure 4 shows that 3D plots of ε' and ε'' as a function of temperature and frequency for the isotropic (Iso), nematic (N) and crystalline (K) phases for 98 wt % 5CB/benzene mixture. Note that we have also two relaxation processes: processes 1 and 2 and these two processes are already described above. Again, for comparison of the phase transitions obtained from DSC, the dielectric study for two different concentrations of 5CB (e.g., 90 and 98 wt % of 5CB) are shown in Fig. 5. One can see from this figure that the relaxation parameters obtained from process 1 ($\Delta\varepsilon_1$, τ_1, and β_1) and from process 2 ($\Delta\varepsilon_2$, τ_2, and β_2) are strongly

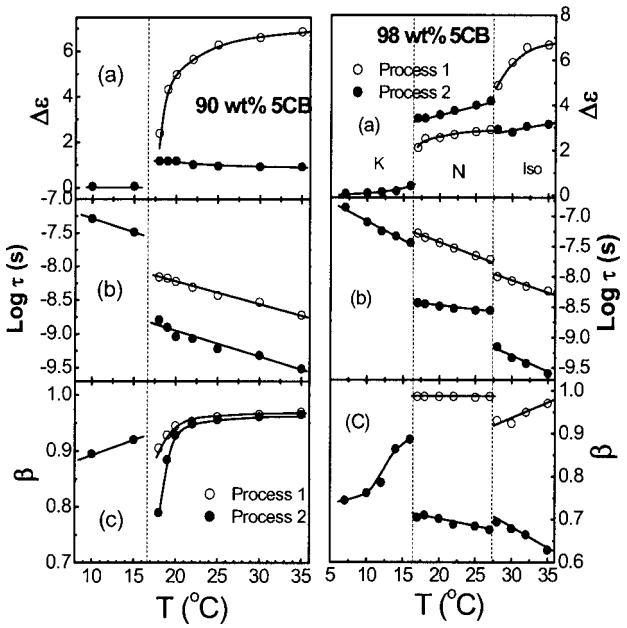

FIG. 5. Temperature dependences of the (a) relaxation strength, (b) relaxation time, and (c) shape parameter for 90 wt % (left figure) and 98 wt % (right figure) of 5CB/benzene mixtures. K, N, and Iso correspond to the crystallization, nematic, and isotropic phases, respectively. The lines are drawn as a guide for the eye.

temperature dependent. However, K–Iso phase transition for 90 wt % of 5CB and K–N and N–Iso phase transitions for 98 wt % of 5CB are described very accurately from the discontinuous nature of each relaxation parameters obtained from each relaxation processes. In the N and Iso phases, we have observed processes 1 and 2 both but in the K phase, the process 1 has disappeared and the relaxation time that is similar with process 2, but even smaller than process 1, showed a discontinuity at the freezing temperature. The relaxation time is larger than those obtained in the nematic phase because of the large restrictions in the crystalline phase. Because the molecular motion of 5CB takes a different mode of dynamics below the freezing point and indicates a characteristic feature of large relaxation time where the anisotropic shape brings a large excluded volume effect in the molecular rotation around the short axis. Therefore, the benzene molecules reduce the molecular interactions with 5CB molecules and the rotational motion around the short axis is strongly restricted and disappears at the freezing temperature, at which temperature benzene and/or 5CB molecules are partially crystallized. This could be due to the formation of a eutectic type crystal structure[38,39] which is composed of benzene and LC molecules. On the other hand, the motion around the longer axis is also affected partially by surrounding medium, because it has a smaller excluded volume. Therefore, this motion is still active even below the freezing temperature. This unfreezable 5CB and benzene molecules are restricted by partially crystallized 5CB and benzene molecules. A discontinuous behavior of the relaxation time for 5CB dynamics at the crystallization temperature results from the abrupt decrease in the volume per one 5CB molecule, compared with that required as the excluded

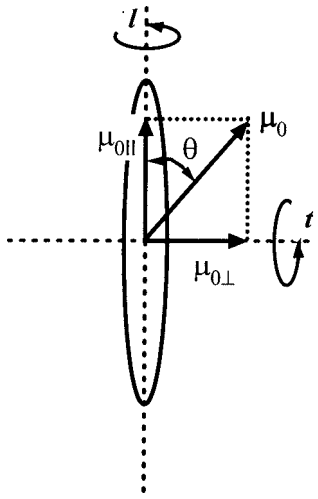

FIG. 6. Schematic representation of the molecular rotations and the dipole moment vectors. Here, μ_0 is the dipole moment vector, θ is the angle between μ_0 and the long axis l, and $\mu_{0\parallel}$ and $\mu_{0\perp}$ are the parallel and perpendicular components of μ_0, respectively.

volume effect.[40] Note that similar behavior was observed for all other concentrations which are not shown in this paper.

We have also evaluated the angle (θ) of dipole moment between the dipole moment vector μ_0 and the long axis l (see Fig. 6) from the ratio of dielectric amplitude of the two relaxation processes for 5CB/benzene mixtures, where $\theta=\tan^{-1}(\Delta\varepsilon_{\text{process 2}}/\Delta\varepsilon_{\text{process 1}})^{1/2}$. This angle depends on the conformation of the flexible alkyl chain with the rigid cyanobiphenyl group (see inset of Fig. 7). Alkyl chain can easily change angles with the rigid cyanobiphenyl group in solution. The mobility of the alkyl chain is freer in the low concentration regions than the higher concentration regions. Figure 7 shows that, below 70 wt % of 5CB, angle of dipole moment between the dipole moment vector μ_0 and the long axis l is almost constant but above 70 wt % of 5CB, the angle of dipole moment between the dipole moment vector μ_0 and the long axis l increases. So, one can say that the dipole moment along the long axis ($\mu_{0\parallel}$) decreases and the dipole moment along the short axis ($\mu_{0\perp}$) increases. The parallel ($\mu_{0\parallel}$) and perpendicular ($\mu_{0\perp}$) components of the

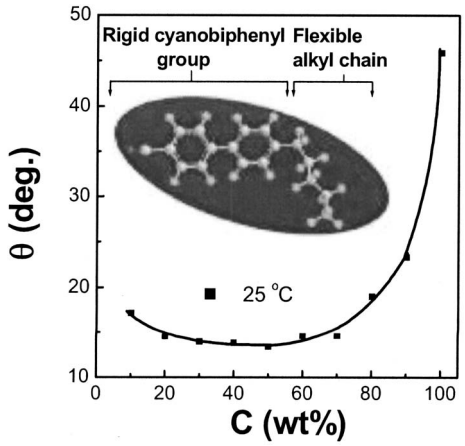

FIG. 7. Concentration dependence of the angle of dipole moment between the short and long axes observed on 5CB/benzene mixture at 25 °C. The lines are drawn as a guide for the eye.

dipole moment vector μ_0 has been shown in Fig. 6. For 100% of 5CB, the rotational motions around the long molecular axis of 5CB is more active to dielectric properties than that around the short molecular axis because of the large dipole moment on the short axis of the rigid cyanobiphenyl group. Antiparallel alignment also affects to decrease the moment on the long axis.

For the 5CB/benzene mixtures, the effective molecular dipole moment can be estimated from the dielectric spectra using[41,42]

$$\mu^2 = \frac{3\varepsilon_0 k_B T}{F}\frac{V}{N}\Delta\varepsilon, \tag{2}$$

with

$$F = \frac{\varepsilon_S(\varepsilon_\infty + 2)^2}{3(2\varepsilon_S + \varepsilon_\infty)},$$

and where $\Delta\varepsilon = \varepsilon_s - \varepsilon_\infty$, ε_s is the static dielectric constant, N is the number of dipoles within volume V in the system, and k_B is the Boltzmann constant. The number density of dipoles N/V is expressed by $\rho N_A/M$. M is the molar mass of the molecules, ρ is the density of 5CB in the system, and N_A is the Avogadro number. Density of pure 5CB is 1.008 g/cm^3 at 25 °C. With the addition of benzene, the concentration of 5CB decreases to zero and the density of the mixtures decreases almost linearly to 0.8786 g/cm^3 (density of benzene). The Kirkwood correlation factor,[43–45] g, $[=(\mu/\mu_0)^2]$ has been obtained for 5CB/benzene mixture, where μ_0 [= 4.85 D (literature value[46])] is the mean square dipole moment for noninteracting isolated dipoles. The parallel and perpendicular components of μ_0 have been calculated by using $\mu_{0\|} = \mu_0 \cos\theta$ and $\mu_{0\perp} = \mu_0 \sin\theta$.[28]

Figure 8 shows the concentration dependence of the dipole moments and the Kirkwood correlation factor for the two relaxation processes observed on 5CB/benzene mixture at 25 °C. From Fig. 8(a), we observe that the rotation of the molecules around the molecular short axis decreases due to decrease in the longitudinal dipole moment with increasing concentration of 5CB. But at high concentration regions (≥70 wt % of 5CB), the dipole moment decreases suddenly, because LC molecules are restricted at concentrations ≥70% of 5CB and also affected by antiparallel alignment. The rotation of the molecules around the molecular long axis arises due to the fact that the transverse dipole moment is almost constant with increasing concentration of 5CB, but at high concentration region (≥70 wt % of 5CB), the dipole moment increases. This behavior of dipole moment is similar to the observed nature of the shape parameter β [Fig. 3(c)], where $\beta = 1$ below 70 wt % of 5CB and $\beta < 1$ at concentrations ≥70 wt % of 5CB. The Kirkwood correlation factor g is closely related to the dipole moment obtained from both the processes 1 and 2. For the process 1, we see that when the concentration is <15 wt % of 5CB, the intermolecular interactions are very week, so that the molecules are free to rotate around their own axis due to the transverse dipole moment [see Fig. 8(b)]. Below 70 wt % of 5CB, the intermolecular interaction increases, i.e., "g" decreases. But at 70 wt % of 5CB, "g" decreases suddenly, i.e., the intermolecular interaction appears to be very strong so that K–Iso phase transition temperature increases suddenly. Above 70 wt % of 5CB, the intermolecular interaction is so stronger that the "g" decreases further. For the process 2, the dipole moment and "g" show opposite nature, because the antiparallel alignments eliminate the dipole moment on the long axis, but the moment on the short axis does not decrease due to the small excluded volume effect at least in the solution, and therefore the transverse dipole moment increases even for pure LC. Note that the large angle θ, obtained for pure LC (see Fig. 7), reflects not only conformation of LC but also the formation of antiparallel alignments. The "g" value also quantifies the behavior of dipole moments, where, "g" being <1 for antiparallel correlation, =1 for no correlation, and >1 for parallel correlation.[47,48] Moreover, the "g" value observed from process 2, appeared due to the fact that the transverse dipole moment is almost similar but the intermolecular interaction is weaker than process 1. This is because the molecular rotation around long axis is easier than the short axis so that the interaction between molecules rotating along the long axis is lower than the short axis.

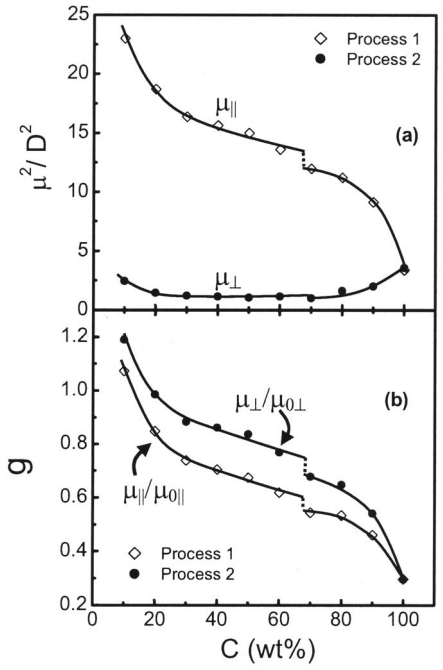

FIG. 8. Concentration dependences of (a) dipole moments and (b) correlation factors for the two relaxation processes observed on 5CB/benzene mixture at 25 °C. The lines are drawn as a guide for the eye.

CONCLUSION

The physical properties of liquid crystal/benzene mixtures were measured very precisely as a function of concentration, temperature, and frequency. The concentration- and temperature-dependent dielectric constants of 5CB clearly showed the successive phase transitions from K to Iso phases. The nematic phase was found when the concentration of 5CB was above 96 wt % of 5CB. Below 96 wt % of 5CB, the nematic phase was absent. For all concentrations, two relaxation processes (processes 1 and 2) were observed

in both N and Iso phases but in the crystalline phase, only process 2 was found. K–N and N–Iso phase transitions were discontinuous as found from the temperature dependence of the relaxation time, relaxation strength, and also from the shape parameters obtained from the fitting procedure of Eq. (1). Alignment of liquid crystalline molecules was observed due to the intermolecular interactions. Antiparallel dimmers of the liquid crystalline molecules were formed in the range between 70 and 96 wt % of 5CB. In the range above 96 wt % of 5CB, the molecular alignments were generated to form a liquid crystalline phase. The intermolecular interactions and the Kirkwood correlation factor, "*g*," between LC and benzene were analyzed. A small change in molecular structure generated in a dramatic change in the corresponding LC properties.

ACKNOWLEDGMENTS

This work was supported by the Japan Society for the promotion of Science (JSPS) (No. 17-05061) and the Ministry of Education, Science, Sports and Culture, Grant-in-Aid for Scientific Research on Priority Areas "Water and Biomolecules" (No. 18031034).

[1] *Liquid Crystals in Complex Geometries Formed by Polymer and Porous Networks*, edited by G. P. Crawford and S. Zumer (Taylor & Francis, London, 1996).
[2] F. M. Aliev, *Access to Nanoporous Materials* (Plenum, New York, 1995).
[3] S. Granick, Science **253**, 1374 (1991).
[4] J. Leys, G. Sinha, C. Glorieux, and J. Thoen, Phys. Rev. E **71**, 051709 (2005).
[5] T. Bellini, L. Radzihovsky, J. Toner, and N. J. Clark, Science **294**, 1074 (2001).
[6] A. Jakli, S. Borbely, and L. Rosta, Eur. Phys. J. B **10**, 509 (1999).
[7] P. G. de Gennes, *Physics of Liquid Crystals* (Oxford University Press, Oxford, 1974).
[8] H. R. Zeller, Phys. Rev. Lett. **48**, 334 (1982).
[9] B. Jérôme, J. O'Brien, Y. Ouchi, C. Stanners, and Y. R. Shen, Phys. Rev. Lett. **71**, 758 (1993).
[10] L. M. Blinov and V. G. Chigrinov, *Electrooptic Effects in Liquid Crystal Materials* (Springer, New York, 1994), p. 138.
[11] J. Jadżyn, G. Czechowski, and M. Ginovska, Phys. Rev. E **71**, 052702 (2005).
[12] N. Usol'tseva, K. Praefcke, D. Singer, and B. Gündogan, Liq. Cryst. **16**, 601 (1994).
[13] G. Hoppke, D. Krüerke, M. Müller, and H. Bobk, Ferroelectrics **179**, 203 (1996).
[14] G. Cinacchi, J. Phys. Chem. B **109**, 8125 (2005).
[15] P. G. Cummins, D. A. Danmur, and D. A. Laidler, Mol. Cryst. Liq. Cryst. **30**, 109 (1975).
[16] D. Lippens, J. P. Parneix, and A. Chapoton, J. Phys. (Paris) **38**, 1465 (1977).
[17] J. M. Wacrenier, C. Druon, and D. Lippens, Mol. Phys. **43**, 97 (1981).
[18] T. K. Bose, R. Chahine, M. Merabet, and J. Thoen, J. Phys. (Paris) **45**, 11329 (1984).
[19] T. K. Bose, B. Campbell, S. Yagihara, and J. Thoen, Phys. Rev. A **36**, 5767 (1987).
[20] A. Buka and A. H. Price, Mol. Cryst. Liq. Cryst. **116**, 187 (1985).
[21] H.-G. Kreul, S. Urban, and A. Würflinger, Phys. Rev. A **45**, 8624 (1992).
[22] W. Haase, Z. X. Fan, and H. J. Müller, J. Chem. Phys. **89**, 3317 (1988).
[23] S. Hauptmann, T. Mosell, S. Reiling, and J. Brickmann, Chem. Phys. **208**, 57 (1996).
[24] M. J. Cook and M. R. Wilson, Liq. Cryst. **27**, 1573 (2000).
[25] C. Amovilli, I. Cacelli, S. Campanile, and G. Prampolini, J. Chem. Phys. **117**, 3003 (2002).
[26] H.-G. Kreul, S. Urban, and A. Würflinger, Phys. Rev. A **45**, 8624 (1992).
[27] T. Shioda, Y. Okada, Y. Takanishi, K. Ishikawa, B. Park, and H. Takezoe, Jpn. J. Appl. Phys. **44**, 3103 (2005).
[28] J. Jadżyn, P. Kędziora, L. Hellemans, and K. De Smet, Chem. Phys. Lett. **302**, 337 (1999).
[29] G. Sinha, J. Leys, C. Glorieux, and J. Thoen, Phys. Rev. E **72**, 051710 (2005).
[30] A. H. Price and D. Davies, J. Chem. Soc., Faraday Trans. **93**, 1775 (1997).
[31] J. Leys, C. Glorieux, M. Wübbenhorst, and J. Thoen, Liq. Cryst. **34**, 749 (2007).
[32] K. De Smet, L. Hellemans, J. F. Rouleau, R. Courteau, and T. K. Bose, Phys. Rev. E **57**, 1384 (1998).
[33] S. Merino, F. de Daran, M. R. de la Fuente, M. A. P. Jubindo, and T. Sierra, Liq. Cryst. **23**, 275 (1997).
[34] S. Merino, M. R. de la Fuente, Y. González, M. A. P. Jubindo, B. Ros, and J. A. Puértolas, Phys. Rev. E **54**, 5169 (1996).
[35] K. S. Cole and R. H. Cole, J. Chem. Phys. **9**, 341 (1941).
[36] S. Takashima, *Electrical Properties of Biopolymers and Membranes* (Hilger, Bristol, 1989).
[37] Y. Hayashi, N. Shinyashiki, and Shin Yagihara, J. Non-Cryst. Solids **305**, 328 (2002).
[38] M. O' Keeffe, Acta Crystallogr., Sect. A: Cryst. Phys., Diffr., Theor. Gen. Crystallogr. **33**, 924 (1977).
[39] K. B. Radhakrishnan and A. R. Balakrishnan, Chem. Eng. Process. **40**, 71 (2001).
[40] S. Yagihara, M. Asano, M. Kosuge, S. Tsubatani, D. Imoto, and N. Shinyashiki, J. Non-Cryst. Solids **351**, 2629 (2005).
[41] L. Onsager, J. Am. Chem. Soc. **58**, 1486 (1938).
[42] C. J. F. Böttcher, *Theory of Electric Polarization* Dielectrics in Static Fields Vol. 1 (Elsevier, Amsterdam, 1973).
[43] J. G. Kirkwood, Ann. N.Y. Acad. Sci. **40**, 315 (1940).
[44] J. G. Kirkwood, Trans. Faraday Soc. **42**, 7 (1946).
[45] J. G. Kirkwood, J. Chem. Phys. **7**, 911 (1939).
[46] K. P. Gueu, E. Megnassan, and A. Proutiere, Mol. Cryst. Liq. Cryst. **132**, 303 (1986).
[47] C. J. F. Böttcher, *Dielectrics in Static Fields*, 2nd ed., Theory of Electric Polarisation Vol. 1 (Elsevier, Amsterdam, 1973).
[48] B. Van Roic, J. Leys, K. Denolf, C. Glorieux, G. Pitsi, and J. Thoen, Phys. Rev. E **72**, 041702 (2005).